Electronic Supplementary Material (ESI) for CrystEngComm

Construction of Lanthanide Metal-Organic Frameworks with Highly-Connected Topology Based on a Tetrapodal Linker

Yun-Shan Xue,[a] Lian Zhou,[a] Mei-Pin Liu, [a] Su-Meng Liu, [a] Yan Xu,[b] Hong-Bin Du[a,*] Xiao-Zeng You[a]

a. State Key Laboratory of Coordination Chemistry, School of Chemistry and Chemical Engineering, Nanjing University, Nanjing, 210093, China.

b. Department of Chemistry, Nanjing University of Technology, Nanjing 210009.

Content

1- Selected bond lengths and angles of compounds **1-3.**

2- Powder X-ray diffraction of compounds **1-3.**

3- Additional TG curves of **1**−**3.**

4- Additional Gas sorption isotherms for compound **1.**

5- Analysis of Gas Sorption Isotherms.

1- Selected bond lengths and angles of compounds 1-3

Table S1 Selected bond lengths (Å) and angles (º) for **1**.

Nd1—O1	2.566(3)	Nd1—O2	2.522(2)
Nd1—O3^{v}	2.475(3)	Nd1—O4^{v}	2.518(2)
Nd1—O5^{vi}	2.496(2)	Nd1—O5^{vii}	2.698(3)
Nd1—O6^{vii}	2.497(2)	Nd1^{ii}—O50^{iv}	2.355(2)
Nd1—O1W	2.458(2)		
O1—Nd1—O1W	142.68(7)	O1—Nd1—O2	51.14(6)
O1—Nd1—O3^{v}	86.54(7)	O1—Nd1—O4^{v}	133.14(7)
O1—Nd1—O5^{vi}	74.51(6)	O1—Nd1—O6^{vii}	75.81(7)
O1—Nd1—O50^{iv}	124.28(7)	O2—Nd1—O1W	145.40(8)
O2—Nd1—O3^{v}	72.66(6)	O2—Nd1—O4^{v}	119.87(6)
O2—Nd1—O5^{vi}	80.91(6)	O2—Nd1—O6^{vii}	118.96(7)
O2—Nd1—O50^{iv}	73.82(7)	O3^{v}—Nd1—O1W	126.99(7)
O3^{v}—Nd1—O50^{iv}	84.75(7)	O4^{v}—Nd1—O1W	74.84(7)
O4^{v}—Nd1—O3^{v}	52.39(6)	O4^{v}—Nd1—O5^{vi}	151.57(7)
O4^{v}—Nd1—O6^{vii}	73.72(7)	O4^{v}—Nd1—O50^{iv}	78.40(7)
O5^{vi}—Nd1—O1W	77.45(7)	O5^{vi}—Nd1—O3^{v}	153.42(6)
O5^{vi}—Nd1—O50^{iv}	90.64(7)	O6^{vii}—Nd1—O1W	94.72(8)
O6^{vii}—Nd1—O3^{v}	76.78(7)	O6^{vii}—Nd1—O5^{vi}	115.09(6)
O6^{vii}—Nd1—O50^{iv}	152.04(8)	O1w—Nd1—O50^{iv}	79.74(8)

Symmetry codes: (i) -0.5+x, 0.5-y, -0.5+z; (ii) -0.5+x, -0.5+y, z; (iii) -0.5+x, 0.5+y, z; (iv) 0.5+x, 0.5+y, z; (v) 0.5+x, 0.5-y, 0.5+z; (vi) 1-x, 1-y, -z; (vii) 0.5+x, -0.5+y, z.

Table S2 Selected bond lengths (Å) and angles (º) for **2.**

Eu1—O1	2.347(3)	Eu1—O5^{iii}	2.337(3)
Eu1—O6^{i}	2.317(3)	Eu1—O1W	2.521(4)
Eu2—O2	2.322(3)	Eu2—O3	2.479(7)
Eu2—O3A	2.434(6)	Eu2—O4	2.367(7)
Eu2—O4A	2.571(7)	Eu2—O2W	2.494(7)
Eu2—O3W	2.712(7)		
O1—Eu1—O1^{v}	88.43(15)	O1—Eu1—O5^{iv}	148.50(11)
O1—Eu1—O5^{iii}	87.27(10)	O1—Eu1—O6^{i}	133.85(11)
O1—Eu1—O6^{ii}	80.44(11)	O5^{iv}—Eu1—O5^{iii}	80.41(14)
O5^{iv}—Eu1—O6^{i}	75.93(11)	O6^{i}—Eu1—O5^{iii}	123.51(11)
O6^{i}—Eu1—O6^{ii}	76.03(16)	O1W—Eu1—O1	73.8(1)
O1W—Eu1—O5^{iii}	75.03(11)	O1W—Eu1—O6^{i}	141.72(8)
O2—Eu2—O2^{v}	77.35(15)	O2—Eu2—O4	147.85(18)
O2—Eu2—O4^{v}	90.45(19)	O3—Eu2—O2^{v}	118.33(19)
O3—Eu2—O2	163.75(19)	O3—Eu2—O3^{v}	45.7(3)
O3—Eu2—O3A	35.3(2)	O3—Eu2—O3A^{v}	74.4(2)
O3—Eu2—O4	43.2(2)	O3—Eu2—O4^{v}	78.0(3)
O3A—Eu2—O2^{v}	89.75(16)	O3A—Eu2—O2	150.98(16)

O3A—Eu2—O3A^{v}	89.4(3)	O4—Eu2—O3A	56.2(2)
O4—Eu2—O3A^{v}	112.8(2)	O4—Eu2—O4^{v}	84.3(4)
O4A—Eu2—O2^{v}	68.73(18)	O4A—Eu2—O2	145.29(18)
O4A—Eu2—O3	50.9(2)	O4A—Eu2—O3^{v}	96.1(2)
O4A—Eu2—O3A	39.0(2)	O4A—Eu2—O3A^{v}	123.8(2)
O4A—Eu2—O4	30.9(2)	O4A—Eu2—O4^{v}	114.5(3)
O4A—Eu2—O2W	84.50(18)	O4A^{v}—Eu2—O2^{v}	145.29(18)
O4A^{v}—Eu2—O2	68.73(18)	O4A^{v}—Eu2—O4	114.5(3)
O4A^{v}—Eu2—O4A	142.9(3)	O2W—Eu2—O2	86.10(14)
O2W—Eu2—O3	98.6(2)	O2W—Eu2—O3A	119.24(17)
O2W—Eu2—O4	63.22(19)	O3W—Eu2—O2	85.89(13)
O3W—Eu2—O3	90.9(2)	O3W—Eu2—O3A	67.13(17)
O3W—Eu2—O4	123.25(19)	O3W—Eu2—O4A	98.53(18)
O3W—Eu2—O2W	169.7(2)		

Symmetry codes: (i) x, -y, -0.5-z; (ii) x, -y, 0.5+z; (iii) 0.5-x, 0.5+y, 0.5+z; (iv) 0.5-x, 0.5+y, -0.5-z; (v) x, y, -z.

Table S3 Selected bond lengths (Å) and angles (º) for **3.**

Er1—O1	2.298(3)	Er2—O2	2.246(4)
Er1—O5^{iii}	2.263(3)	Er2—O3	2.392(9)
Er1—O6^{i}	2.259(4)	Er2—O3A^{v}	2.346(7)
Er1—O1W	2.390(5)	Er2—O3A	2.346(7)
Er2—O4	2.327(10)	Er2—O4A^{v}	2.473(8)
Er2—O2W	2.374(6)	Er2—O3W	2.449(9)
O1^{v}—Er1—O1	86.84(17)	O2—Er2—O2^{v}	78.33(18)
O1^{v}—Er1—O1W	74.10(13)	O2—Er2—O3^{v}	117.7(3)
O5^{iii}—Er1—O1	87.93(13)	O2^{v}—Er2—O3^{v}	163.4(2)
O5^{iv}—Er1—O1	150.12(15)	O2—Er2—O3A^{v}	88.3(3)
O5^{iv}—Er1—O1W	76.17(14)	O2^{v}—Er2—O3A^{v}	153.5(3)
O6^{i}—Er1—O1^{v}	129.96(14)	O2—Er2—O4^{v}	92.9(4)
O6^{ii}—Er1—O1^{v}	79.01(14)	O2—Er2—O4	147.0(2)
O6^{i}—Er1—O5^{iii}	77.50(15)	O2—Er2—O4A	147.4(2)
O6^{i}—Er1—O5^{iv}	125.44(14)	O2^{v}—Er2—O4A	70.9(2)
O6^{ii}—Er1—O5^{iv}	77.50(15)	O2—Er2—O2W	78.46(16)
O5^{iii}—Er1—O5^{iv}	82.15(17)	O2—Er2—O3W	86.25(15)
O6^{i}—Er1—O6^{ii}	74.6(2)	O3^{v}—Er2—O3	46.0(5)
O6^{i}—Er1—O1W	142.7(1)	O3^{v}—Er2—O4A	93.9(4)
O3A^{v}—Er2—O3^{v}	34.5(4)	O3—Er2—O4A	49.1(3)
O3A—Er2—O3^{v}	75.4(3)	O3—Er2—O3W	90.7(5)
O3A^{v}—Er2—O3A	94.2(5)	O4^{v}—Er2—O4	77.2(7)
O3A^{v}—Er2—O4A^{v}	37.5(3)	O4^{v}—Er2—O4A	106.9(5)
O3A—Er2—O4A^{v}	124.3(4)	O4—Er2—O4A	30.2(3)
O3A^{v}—Er2—O2W	121.4(3)	O4—Er2—O2W	68.6(3)
O3A^{v}—Er2—O3W	70.0(3)	O4—Er2—O3W	125.2(2)

O4^{v}—Er2—O3^{v}	42.6(4)	O4A—Er2—O4A^{v}	135.5(5)
O4—Er2—O3^{v}	75.6(4)	O2W—Er2—O3^{v}	107.5(5)
O4^{v}—Er2—O3A^{v}	55.2(3)	O2W—Er2—O4A	84.9(3)
O4—Er2—O3A^{v}	110.1(4)	O2W—Er2—O3W	160.2(2)
O3W—Er2—O4A	102.0(3)		

Symmetry codes: (i) x, -y, 0.5+z; (ii) x, -y, -0.5-z; (iii) 0.5-x, 0.5+y, 0.5+z; (iv) 0.5-x, 0.5+y, -0.5-z; (v) x, y, -z.

2- Powder X-ray diffraction of compounds 1-3

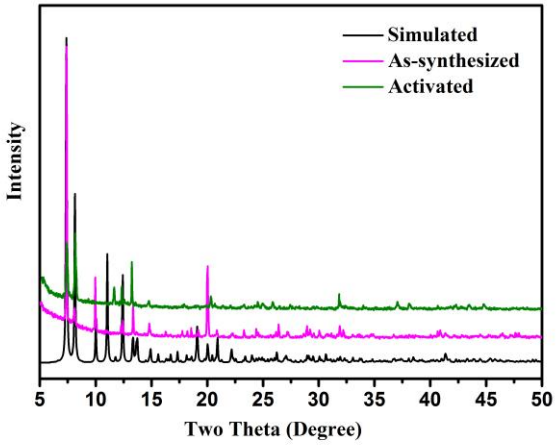

Figure S1. X-ray powder diffraction patterns of compound **1**.

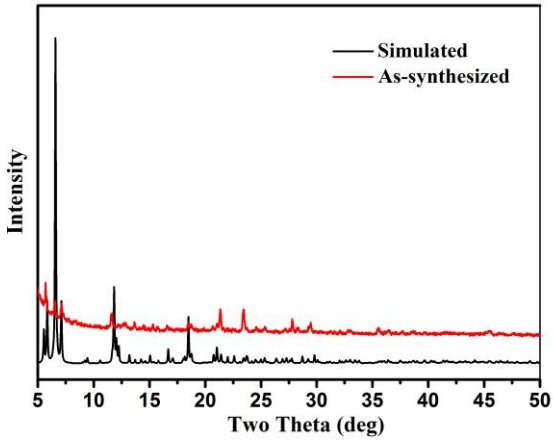

Figure S2. X-ray powder diffraction patterns of compound **2**.

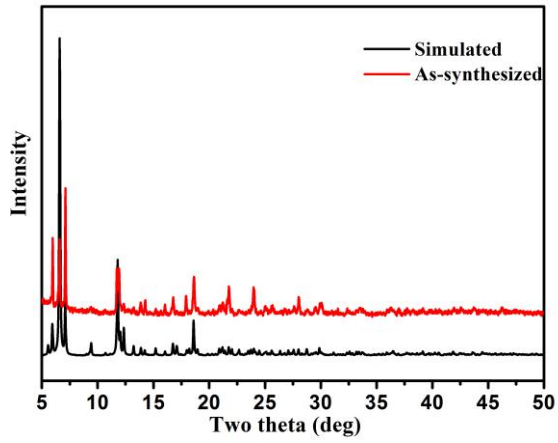

Figure S3. X-ray powder diffraction patterns of compound **3**.

3- Additional TG curves of 1−3.

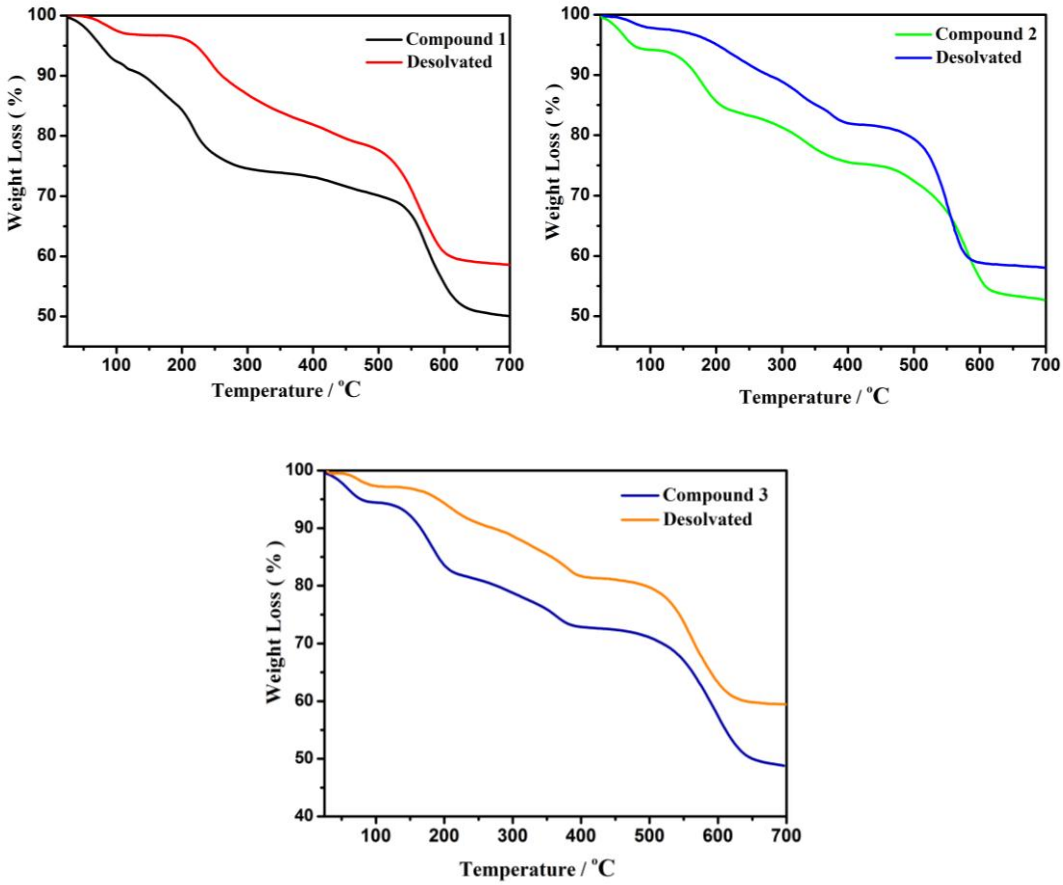

Figure S4. TGA profiles under nitrogen for compounds **1-3.**

4- Additional Gas sorption isotherms for compound 1

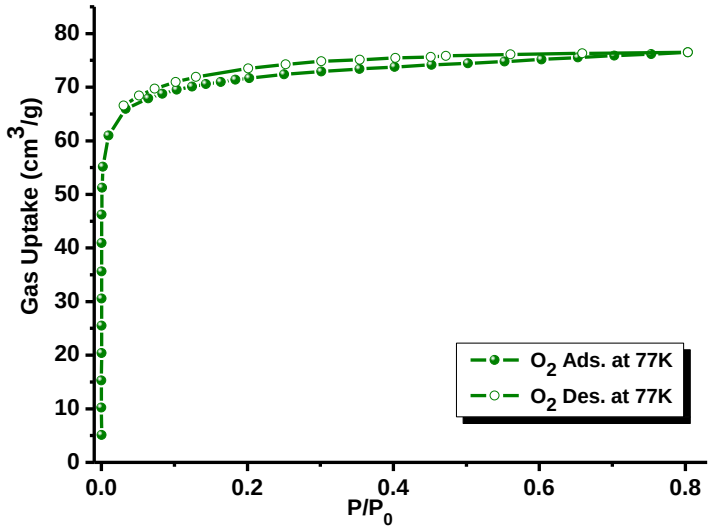

Figure S5. Gas sorption isotherms of **1** for O_2 at 77 K.

5- Analysis of Gas Sorption Isotherms.

Several isotherm models were tested to fit the experimental pure isotherms for CO_2 and CH_4, and the dual-site Langmuir-Freundlich equation was found to best fit the experimental data according to the literature.[S1]

$$q = qm1 \times \frac{b1 \times P^{1/n1}}{1 + b1 \times P^{1/n1}} + qm2 \times \frac{b2 \times P^{1/n2}}{1 + b2 \times P^{1/n2}} \qquad (\mathrm{I})$$

Here, P is the pressure of the bulk gas at equilibrium with the adsorbed phase (kPa), q is the adsorbed amount per mass of adsorbent (mmol/g), q_{m1} and q_{m2} are the saturation capacities of sites 1 and 2 (mmol/g), b_1 and b_2 are the affinity coefficients of sites 1 and 2 (1/kPa), and n_1 and n_2 represent the deviations from an ideal homogeneous surface.

Equation (I) rearranges to:

$$y = P1 \times \frac{P2 \times x^{P3}}{1 + P2 \times x^{P3}} + P4 \times \frac{P5 \times x^{P6}}{1 + P5 \times x^{P6}} \qquad (\mathrm{II})$$

(1) Fitting CH_4 adsorption isotherms using the dual-site Langmuir-Freundlich equation

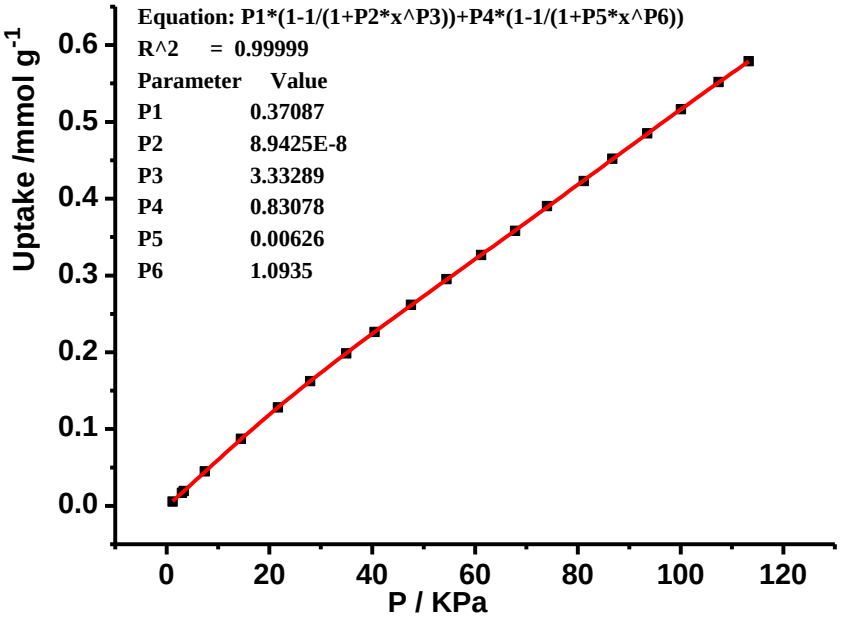

(2) Fitting CO_2 adsorption isotherms using the dual-site Langmuir-Freundlich equation

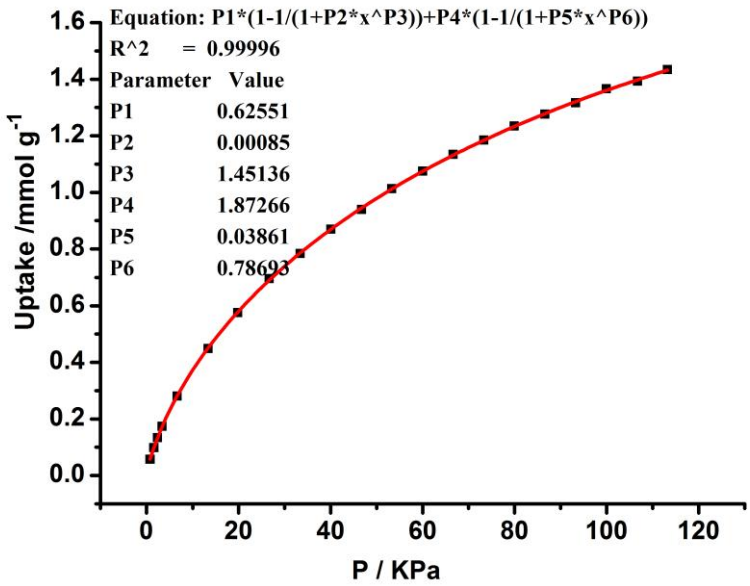

(3) The IAST-predicted isotherms and selectivities of equimolar mixtures of CO_2 and CH_4 at 273 K. The selectivity $S_{CO2/CH4}$ in a binary mixture of components CO_2 and CH_4 is defined as $(x_{CO2}/y_{CO2})/(x_{CH4}/y_{CH4})$, where x_i and y_i are the mole fractions of component i (i = CO_2, CH_4) in the adsorbed and bulk phases, respectively.

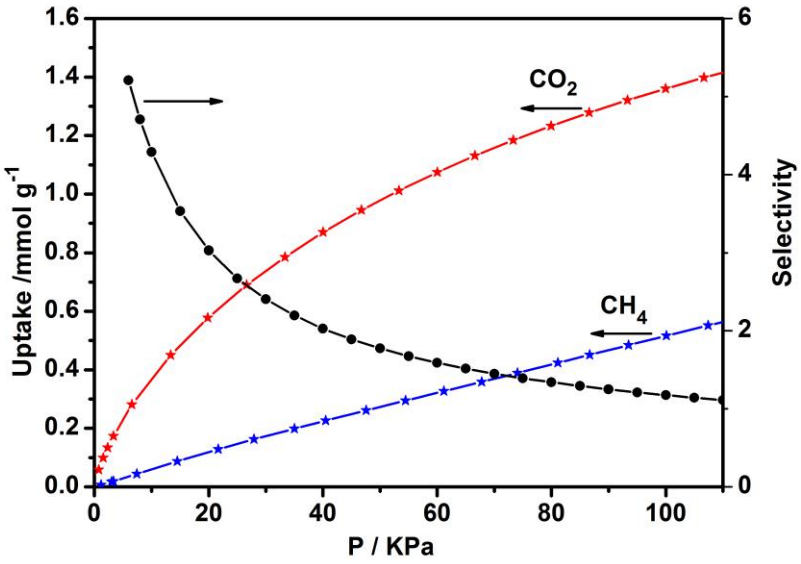

Figure S6. IAST selectivity of CO_2 over CH_4 at 273K.

Reference:

S1. Y. S. Bae, K. L. Mulfort, H. Frost, P. Ryan, S. Punnathanam, L. J. Broadbelt, J. T. Hupp, R. Q. Snurr, *Langmuir*, 2008, **24**, 8592.